

# Empirical Improvements for Estimating Earthquake Response Spectra with Random-Vibration Theory

by David M. Boore and Eric M. Thompson

**Abstract** The stochastic method of ground-motion simulation is often used in combination with the random-vibration theory to directly compute ground-motion intensity measures, thereby bypassing the more computationally intensive time-domain simulations. Key to the application of random-vibration theory to simulate response spectra is determining the duration ( $D_{\text{rms}}$ ) used in computing the root-mean-square oscillator response. Boore and Joyner (1984) originally proposed an equation for  $D_{\text{rms}}$ , which was improved upon by Liu and Pezeshk (1999). Though these equations are both substantial improvements over using the duration of the ground-motion excitation for  $D_{\text{rms}}$ , we document systematic differences between the ground-motion intensity measures derived from the random-vibration and time-domain methods for both of these  $D_{\text{rms}}$  equations. These differences are generally less than 10% for most magnitudes, distances, and periods of engineering interest. Given the systematic nature of the differences, however, we feel that improved equations are warranted. We empirically derive new equations from time-domain simulations for eastern and western North America seismological models. The new equations improve the random-vibration simulations over a wide range of magnitudes, distances, and oscillator periods.

*Online Material:* SMSIM parameter files, tables of coefficients and model parameters, and shaded contour plots of TD/RV ratios for two WNA models.

## Introduction

The stochastic method (Boore, 2003) is widely used for the simulation of seismic ground-motion intensity measures (GMIMs), such as peak acceleration and response spectral amplitudes, particularly for regions lacking strong-motion recordings for magnitudes and distances of engineering interest. Recent applications include the ongoing PEGASOS Refinement Project in Switzerland (Abrahamson *et al.*, 2002; Renault *et al.*, 2010) and the Pacific Earthquake Engineering Research (PEER) Center's Next Generation Attenuation–East (NGA-E) project (see Data and Resources section). The GMIMs can be simulated using either time-domain (TD) or random-vibration (RV) simulations, given the model describing the Fourier spectrum of ground motion (this spectrum includes source radiation effects and the amplitude changes due to propagation from the source to the site) and a description of the duration of ground shaking at the site (which is made up of source and path contributions; this duration of excitation is denoted here as  $D_{\text{ex}}$ ). RV simulations are usually thousands of times faster than TD simulations; the shorter computational times are important for computationally intensive applications such as inverting data for model parameters (Scherbaum *et al.*, 2006) or simulating the probability den-

sity distribution of GMIMs by Monte Carlo simulations that sample the probability distributions of the model parameters.

Although the calculations are much quicker, there is a potential fundamental problem with RV simulations: the basic assumptions behind RV calculations, such as quasi stationarity of the equivalent time series and the statistical independence of consecutive maxima of the time series, are not obviously satisfied, particularly for long-period GMIMs. To overcome these limitations, modifications to the RV simulations in which two measures of duration are used were proposed by Boore and Joyner (1984), denoted by BJ84. The measure of most concern to us is  $D_{\text{rms}}$ , the duration used to compute the root mean square (rms) of the oscillator response. BJ84 introduced an equation for  $D_{\text{rms}}$ , and Liu and Pezeshk (1999), denoted by LP99, using BJ84 as the starting point, proposed a different equation. Both the BJ84 and LP99 equations were based on comparisons of TD and RV simulations for the same model, as well as some theoretical considerations. The adequacy of those modifications, however, was demonstrated only for a few magnitudes and distances by comparing response spectra plotted using a log scale for the ordinate. We recently had occasion to look more

carefully at the comparisons for a wide range of magnitudes and distances, using ratios of TD and RV simulations. An example is shown in Figure 1. The stochastic simulations were generated with the SMSIM software (Boore, 2005). The model parameters are given in Table 1 and in the  $\text{\textcircled{E}}$  electronic supplement to this paper, as discussed later. As shown in Figure 1, the results using the LP99 equation are generally better than those using the BJ84 equation, and both are generally much better than using  $D_{\text{ex}}$  in computing the rms of the oscillator response, particularly for magnitudes of 6 and greater. In spite of the improvements obtained using the equations introduced by BJ84 and LP99, there are significant discrepancies from the TD results (which we take to be the correct GMIMs, given the assumed seismological model), particularly at long periods. There is also a consistent, but small, bias at short periods that is essentially independent of magnitude and distance. These discrepancies are hard to see on traditional plots of GMIMs using a log scale for

the ordinate because the GMIMs span a wide range of amplitudes as a function of period for a given magnitude and distance. In this paper, we evaluate the existing  $D_{\text{rms}}$  equations for more magnitudes and distances than were originally used to derive these equations, and from these results we provide improvements to the  $D_{\text{rms}}$  equations for several stochastic-method models. We start with a brief review of the RV method as used in the stochastic method developed by Boore (1983, 2003). This is followed by the main section containing the improved equation for  $D_{\text{rms}}$ .

## Review of RV Simulations

As discussed in Boore (1983, 2003), the RV simulations are based on two things: (1) the rms of the GMIM ( $y_{\text{rms}}$ ), obtained through Parseval's theorem from the seismological-dependent model of the Fourier amplitude spectrum, and (2) a peak-to-rms factor ( $p = y_{\text{max}}/y_{\text{rms}}$ ), relating the

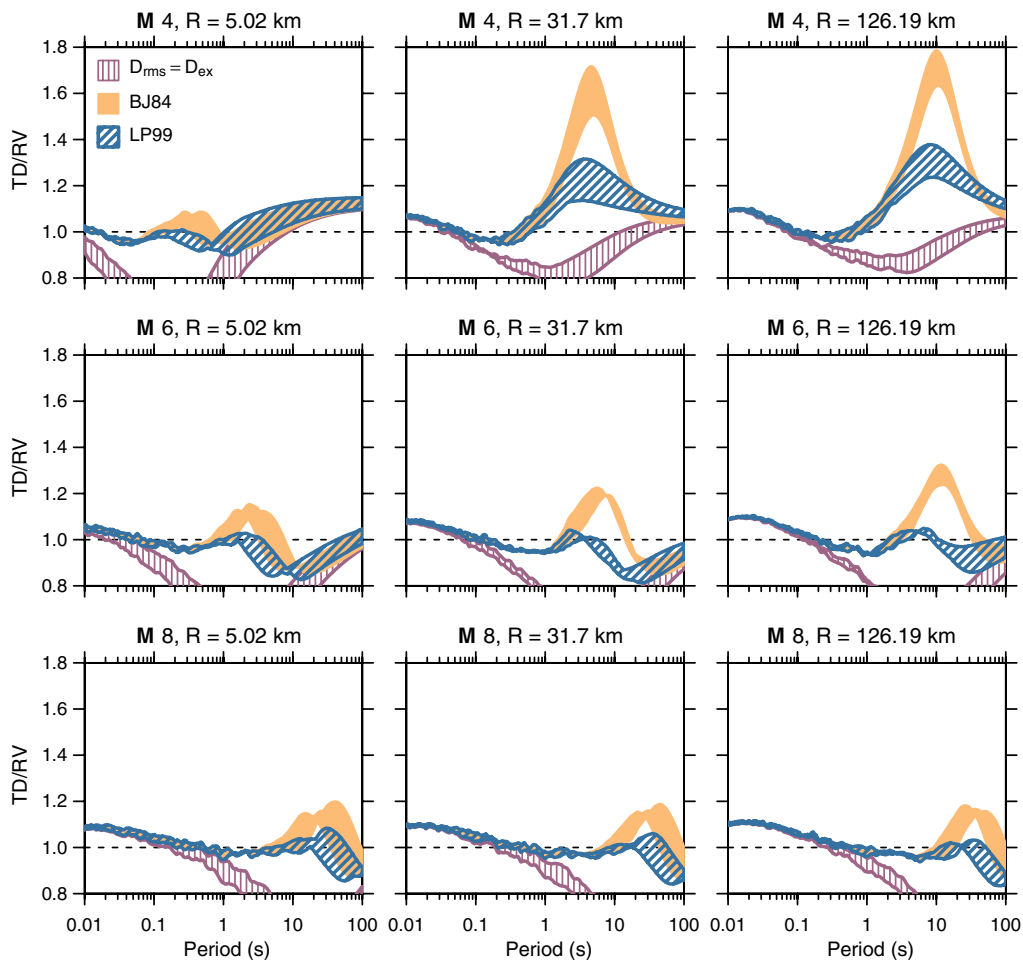


**Figure 1.** Ratios of the pseudoabsolute response spectral acceleration (PSA) computed from TD simulations to the PSA computed with random vibration theory using the BJ84 and LP99  $D_{\text{rms}}$  equations for different magnitudes and distances, and using the ENA model given in Table 1 with no low-cut filter. Also shown is the TD/RV ratio when  $D_{\text{rms}} = D_{\text{ex}}$  (i.e., no RV modification to account for the oscillator response). The ordinate scale was chosen deliberately to emphasize the results using BJ84 and LP99, at the expense of truncating the TD/RV ratios for the  $D_{\text{rms}} = D_{\text{ex}}$  case, which have minimum values near 0.6. Note that the shaded regions encompass the range of ratios obtained for three different stresses: 62.4, 250, and 1000 bars. The color version of this figure is available only in the electronic edition.

Table 1  
Essential Differences in the Stochastic-Method Models Used in the Simulations Discussed in This Paper\*

Model	Source	Path Attenuation	Path Duration	$\kappa$ (s)
ENA: SCF	Single-corner frequency	Atkinson (2004)	Atkinson and Boore (2006)	0.005
ENA: AB95	Double-corner frequency (Atkinson and Boore, 1995)	Atkinson (2004)	Atkinson and Boore (2006)	0.005
WNA: SCF	Single-corner frequency	Raof <i>et al.</i> (1999)	0.05R	0.030
WNA: AS00	Double-corner frequency (Atkinson and Silva, 2000)	Raof <i>et al.</i> (1999)	0.05R	0.030

\*See the  electronic supplement to this paper for the parameter files used in the simulations.

peak GMIM ( $y_{\max}$ ) to  $y_{\text{rms}}$ . In this paper, we compute  $p$  using the equations given by Boore (2003), which are based on equation (6.8) in Cartwright and Longuet-Higgins (1956). Another method for computing  $p$  is given by Der Kiureghian (1980). We have compared GMIMs from both methods and do not find that one is better than the other; for the sake of consistency, the oscillator modifications given in this paper should be used with the Boore (2003) computation of  $p$ .

Boore and Joyner (1984) introduced a modification to the RV method for computing response spectra by using different duration measures in computing  $p$  and  $y_{\text{rms}}$ . The duration of ground motion,  $D_{\text{ex}}$ , is used in computing  $p$ , while  $y_{\text{rms}}$  is computed using a modification of  $D_{\text{ex}}$  that accounts for the increase in duration due to oscillator response; this duration is termed  $D_{\text{rms}}$ . This paper is fundamentally concerned with computing  $D_{\text{rms}}$  as a function of magnitude, distance, oscillator period, and the seismological model.

### A New Equation for Computing $D_{\text{rms}}$

A useful equation for determining the  $D_{\text{rms}}$  that will provide agreement between the TD and RV simulations for a given set of model parameters, including oscillator period, magnitude, and distance, is easily derived from the definitions of  $y_{\text{rms}}$  and the rms-to-peak factor  $p$ . From Parseval's theorem,

$$y_{\text{rms}} = \sqrt{m_0/D_{\text{rms}}}, \quad (1)$$

where  $m_0$  is the zeroth spectral moment (e.g., Boore, 2003) and  $D_{\text{rms}}$  is the duration to be used in computing  $y_{\text{rms}}$ . From the definition of  $p$  given in the Review of RV Simulations section, we have

$$y_{\max} = p \times y_{\text{rms}}. \quad (2)$$

As discussed before,  $p$  depends on  $D_{\text{ex}}$ , the duration of ground motion, and not on the duration of the oscillator response. Now consider two estimates of  $y_{\max}$ : one from the TD simulation (assumed to be the correct value) and one from the RV simulation with no adjustment to account for the oscillator response (i.e.,  $D_{\text{rms}} = D_{\text{ex}}$ ). Call them  $y_{\text{td}}$  and  $y_{\text{xo}}$ , respectively. Equations (1) and (2) give

$$y_{\text{td}} = p \times \sqrt{m_0/D_{\text{rms}}} \quad (3)$$

and

$$y_{\text{xo}} = p \times \sqrt{m_0/D_{\text{ex}}}. \quad (4)$$

Because  $p$  is the same in both equations, equations (3) and (4) can be solved for the value of  $D_{\text{rms}}$  that will give the correct value of ground motion when used in the RV simulations:

$$D_{\text{rms}} = D_{\text{ex}}(y_{\text{xo}}/y_{\text{td}})^2 \quad (5)$$

or

$$D_{\text{rms}}/D_{\text{ex}} = (y_{\text{xo}}/y_{\text{td}})^2. \quad (6)$$

To illustrate the use of equation (6), we generated both TD and RV simulations for the models given in Table 1 and  the parameter input files contained in the electronic supplement to this paper. We used the SMSIM software (Boore, 2005) for the simulations. The base model for the illustrations in this paper is the eastern North America (ENA) single-corner frequency (SCF) model (we used this model because an important application of the stochastic method is in deriving ground motions in ENA, as in the ongoing NGA-E project). For each magnitude–distance pair, we use the arithmetic mean of the response spectra of 800 TD simulations as the TD GMIM (we found that such a large number was necessary to obtain relatively smooth pseudoabsolute response spectral acceleration [PSA] when plotted versus period). The motions in Figure 1 considered a range of stress parameters (a factor of 4 on either side of 250 bars), and the results show that the TD/RV ratio is not sensitive to the stress parameter. For that reason, we used 250 bars (see Boore, 2009) and generated  $y_{\text{td}}$  and  $y_{\text{xo}}$  for many values of magnitude, distance, and oscillator period. The results are shown in Figure 2, where  $D_{\text{rms}}/D_{\text{ex}} = (y_{\text{xo}}/y_{\text{td}})^2$  is plotted against both the oscillator period  $T_o$  and the normalized oscillator period  $T_o/D_{\text{ex}}$  for (top row) one distance and many magnitudes and (bottom row) one magnitude and many distances. Using the normalized oscillator period removes much of the apparent variability in  $D_{\text{rms}}/D_{\text{ex}}$ , suggesting that a relatively simple functional form in terms of  $T_o/D_{\text{ex}}$  can be found that will improve upon the BJ84 and LP99 equations for  $D_{\text{rms}}$ .

### Functional Form

The general form of the equation used by BJ84 and LP99 to obtain  $D_{\text{rms}}$  is

$$D_{\text{rms}} = D_{\text{ex}} + D_o \left( \frac{\gamma^n}{\gamma^n + \alpha} \right), \quad (7)$$

where  $\gamma = D_{\text{ex}}/T_o$ .  $D_o$  is the oscillator duration  $T_o/2\pi\zeta$ , where  $\zeta$  is the fractional damping of the oscillator, usually 0.05. As we saw in Figure 2,  $T_o/D_{\text{ex}}$  rather than  $T_o$  is a better predictor variable for  $D_{\text{rms}}/D_{\text{ex}}$ . For this reason, we rewrite equation (7) as

$$D_{\text{rms}}/D_{\text{ex}} = 1 + \frac{1}{2\pi\zeta} \left( \frac{\eta}{1 + \alpha\eta^n} \right), \quad (8)$$

where  $\eta = T_o/D_{\text{ex}}$ . BJ84 recommend  $n = 3$  and  $\alpha = 1/3$ . LP99 recommend  $n = 2$  and  $\alpha$  to be determined from an equation that accounts for spectral shape. Equation (8) has the property that  $D_{\text{rms}}/D_{\text{ex}}$  approaches unity for small and large values of  $\eta$  for  $n > 1$ . These are physical constraints that follow from the oscillator time series being proportional to the ground acceleration and ground displacement at short and long periods, respectively, and therefore the duration of the oscillator response will be equal to the duration of the ground motion at these asymptotic values of period. But Figure 2 shows that  $D_{\text{rms}}/D_{\text{ex}}$  does not always approach unity, and in many cases it approaches a different value as  $\eta$  approaches zero than when  $\eta$  approaches infinity.  $D_{\text{rms}}/D_{\text{ex}}$

is given by the ratio of RV to TD simulations (equation 6), and thus the fact that  $D_{\text{rms}}/D_{\text{ex}}$  does not approach the theoretical value of unity indicates a bias between the RV and TD simulations. To allow for the empirical observation that  $D_{\text{rms}}/D_{\text{ex}}$  does not approach unity for small and large values of  $\eta$ , we add a term to equation (8) to get

$$D_{\text{rms}}/D_{\text{ex}} = \left( c_1 + c_2 \frac{1 - \eta^2}{1 + \eta^2} \right) \left[ 1 + \frac{1}{2\pi\zeta} \left( \frac{\eta}{1 + \alpha\eta^n} \right) \right], \quad (9)$$

which approaches  $c_1 + c_2$  as  $\eta$  approaches zero and  $c_1 - c_2$  as  $\eta$  approaches infinity. This equation is still not general enough to capture the range in shapes of  $D_{\text{rms}}/D_{\text{ex}}$  that we observe, so we further generalize the equation by allowing  $\alpha$  and  $n$  to be free coefficients ( $c_5$  and  $c_6$ , respectively) to be estimated from the data and by adding three more coefficients ( $c_3$ ,  $c_4$ , and  $c_7$ ):

$$D_{\text{rms}}/D_{\text{ex}} = \left( c_1 + c_2 \frac{1 - \eta^{c_3}}{1 + \eta^{c_3}} \right) \left[ 1 + \frac{c_4}{2\pi\zeta} \left( \frac{\eta}{1 + c_5\eta^{c_6}} \right)^{c_7} \right]. \quad (10)$$

This is the equation that we fit to the simulated  $D_{\text{rms}}/D_{\text{ex}}$  ratio, with a set of coefficients for each magnitude and distance.

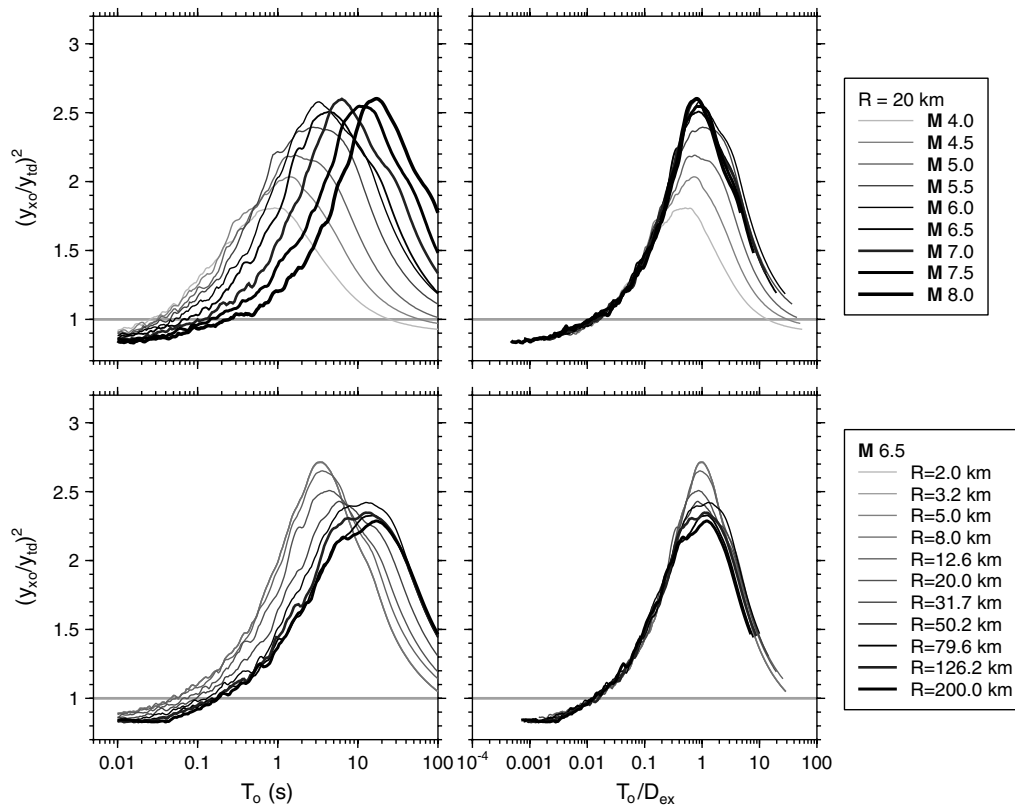


**Figure 2.** Squared ratios of PSA from RV simulations (for which  $D_{\text{rms}} = D_{\text{ex}}$ ) and TD simulations, for the ENA SCF model in Table 1 with 250 bar stress parameter and no low-cut filter, plotted against period ( $T_o$ ) and period normalized by the duration of excitation ( $T_o/D_{\text{ex}}$ ). The top row shows ratios for a fixed distance (20 km) and a range of magnitudes; the bottom row shows ratios for a fixed magnitude (6.5) and a range of distances.

**Table 2**  
The Range of the Parameters in Equation (10) Used in the Genetic Algorithm

Parameter	Minimum	Maximum
$c_1$	0.7	1.2
$c_2$	-0.6	0
$c_3$	2	2
$c_4$	0	3
$c_5$	0	50
$c_6$	1	10
$c_7$	0	10

Estimation of the Coefficients

We used the SMSIM programs `tmrs_loop_rv_drvr` and `tmrs_loop_td_drvr` to generate GMIMs for a set of 15 distances logarithmically spaced from 2 to 1262 km and 9 magnitudes linearly spaced from 4 to 8. For each magnitude–distance pair, we computed PSA at 200 logarithmically spaced periods for 5% damping. We do not provide coefficients for other damping levels because we prefer to

use correlations of PSA for various damping levels, such as those of [Cameron and Green \(2007\)](#) and those being developed for the PEER Next Generation Attenuation–West 2 (NGA-W2) project (see [Data and Resources](#) section), which can be used to adjust for simulations of PSA for other levels of damping. We computed  $D_{rms}/D_{ex}$  for several ENA and western North America (WNA) models, including SCF and double-corner frequency models. An additional consideration is the low-cut filter; we simulated the GMIMs with no low-cut filter and with a low-cut filter frequency ( $f_{lc}$ ) of 0.03 Hz. The illustrations in this article used as a base case the SCF model for ENA with no low-cut filter. The  $D_{rms}/D_{ex}$  ratio depends on whether a box or an exponential window is used in the TD simulations. Because we think that most users prefer the more realistic look of the acceleration time series computed using the exponential window, we only report coefficients for the exponential TD window of [Sara-goni and Hart \(1974\)](#). This was also the window used for the simulations on which the BJ84 and LP99 equations were based.

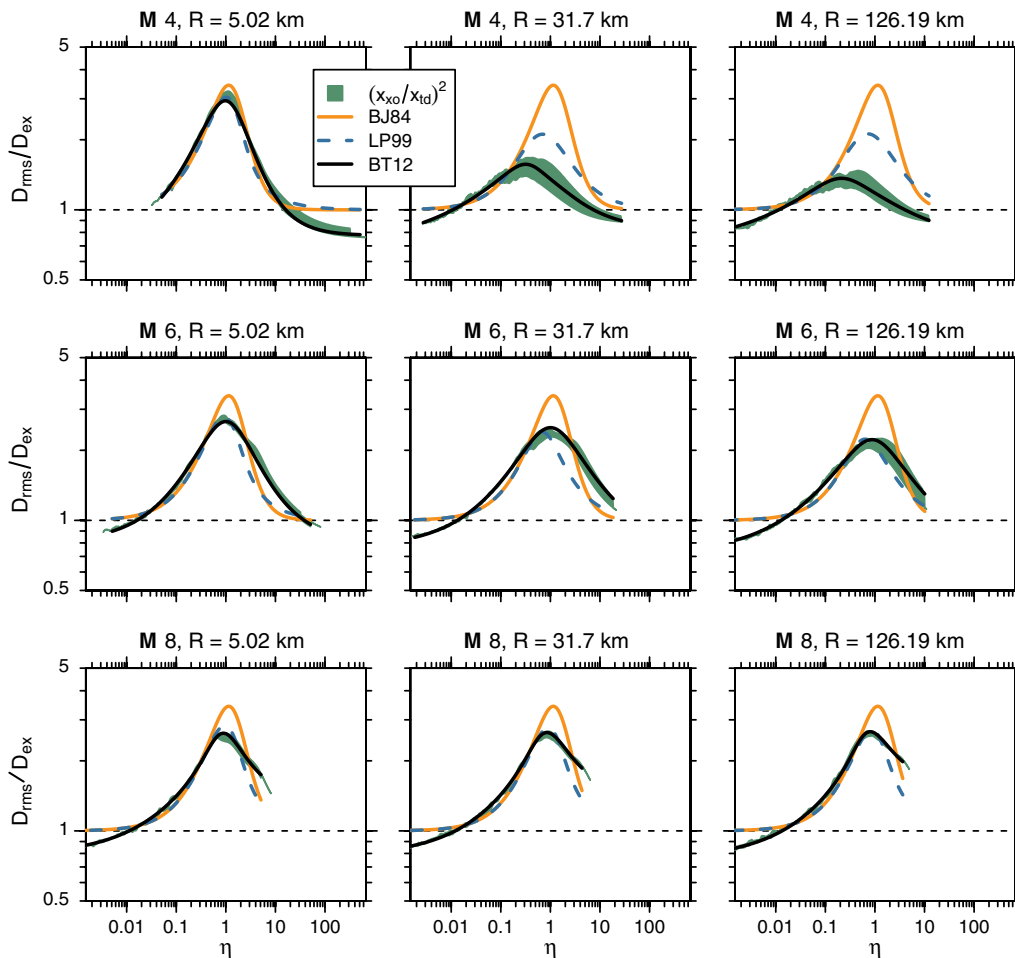


**Figure 3.** Plots of  $D_{rms}/D_{ex}$  as estimated from equation (6), that is,  $(y_{xo}/y_{id})^2$ , as a function of  $\eta = T_o/D_{ex}$  for the same  $M$ ,  $R$ , and stresses as in Figure 1. The BT12 curves are from equation (10), with the coefficients derived from fitting the  $D_{rms}/D_{ex}$  values obtained from the TD and RV simulations. The BJ84 and LP99 curves are from equation (8), with the coefficients recommended by the respective authors. The color version of this figure is available only in the electronic edition.

Given the complex functional form of equation (10), the interdependence of the parameters, and the restricted range of possible values that the parameters may take, we decided to use a genetic algorithm (GA) to search the parameter space for the best values of the coefficients. Given the insensitivity to stress, we defined the misfit relative to  $D_{\text{rms}}/D_{\text{ex}}$  for a single representative stress value for each region (100 bars for WNA, 250 bars for ENA). The ranges of allowable values for the coefficients are listed in Table 2 (based on exploratory calculations, we decided to constrain  $c_3$  to the value 2.0). The GA uses 256 for the population size and the maximum number of generations. For each magnitude–distance bin, we computed two GA estimates of the coefficients, using two seeds to generate initial populations of models, and selected the GA estimate leading to the best fit as the final estimate. The two estimates were (1) using the coefficients from the previous magnitude at the same distance, and (2) using the previous distance at the same magnitude (except for the first magnitude–distance bin, which used the coefficients that simplify equation 10 to the BJ84 equation). We derived coefficients for equation (10) from simulations for the two base-case SCF models for ENA and WNA;  $\text{\textcircled{E}}$  the coefficients are

available in the electronic supplement to this paper. We validated these equations at the midpoints between the magnitudes and distances where the coefficients are defined (geometric midpoints for distance) and found no increase in the misfit to  $D_{\text{rms}}/D_{\text{ex}}$ . For magnitude and distance values not in the coefficient tables, we first compute  $D_{\text{rms}}/D_{\text{ex}}$  for the four tabulated moment magnitude ( $M$ ) and distance ( $R$ ) pairs surrounding the desired  $M$  and  $R$ , and then use bilinear interpolation to obtain  $D_{\text{rms}}/D_{\text{ex}}$ .

### Some Results Using the New Equation

A sample of the simulated and fitted  $D_{\text{rms}}/D_{\text{ex}}$  ratios is given in Figure 3, along with  $D_{\text{rms}}/D_{\text{ex}}$  from the BJ84 and LP99 methods for computing  $D_{\text{rms}}$ . The TD/RV ratios obtained using the new computations of  $D_{\text{rms}}$  (designated by BT12, after the authors' last initials and year of publication of this paper) are shown in Figure 4, which is the same as Figure 1 with the addition of the RV simulations using the BT12 computations. Figure 5 displays a different way of showing the comparison, using shaded contour plots for a wide range of periods and distances for a set of magnitudes and methods

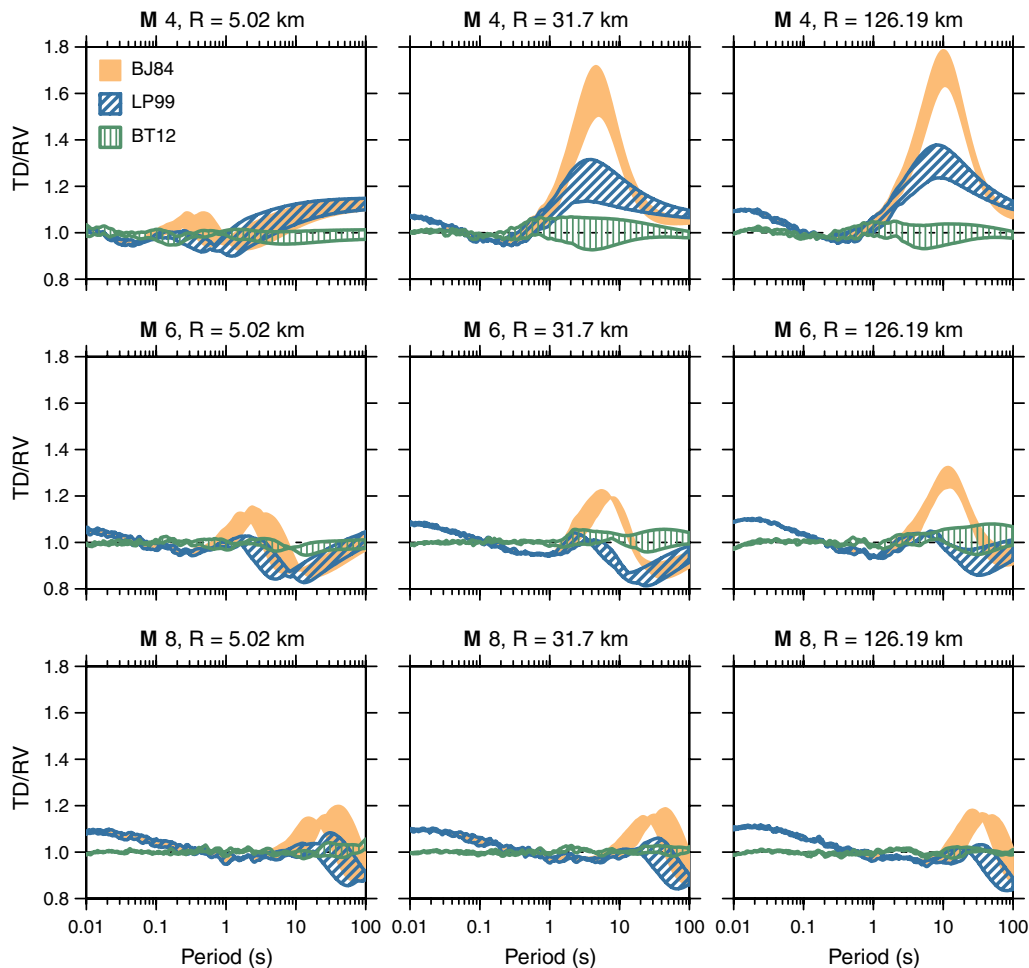


**Figure 4.** Same as Figure 1 with the addition of the ratios computed using the  $D_{\text{rms}}$  equation proposed in this paper (BT12). The color version of this figure is available only in the electronic edition.

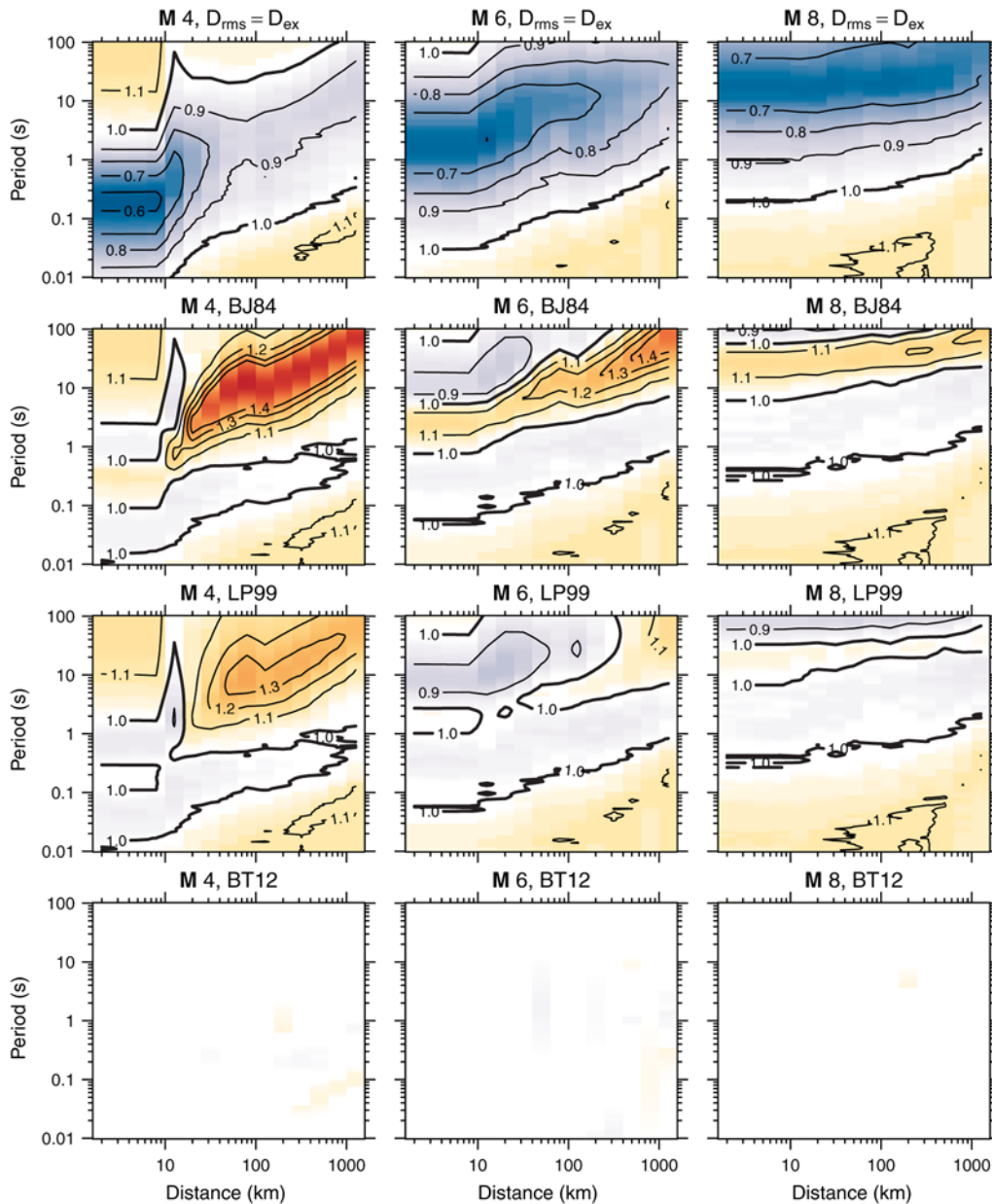


**Figure 5.** A shaded contour plot of the TD/RV ratios for the ENA SCF 250 bar, no low-cut filter model for (top row)  $D_{\text{rms}} = D_{\text{ex}}$  (no modification for an oscillator) and the following models for calculating the  $D_{\text{rms}}$  used in the RV simulations: (second row) BJ84, (third row) LP99, and (bottom row) BT12. The results of using the BT12 calculations of  $D_{\text{rms}}$  look blank because the ratios are within  $\pm 5.3\%$  of unity. The color version of this figure is available only in the electronic edition.

to compute  $D_{\text{rms}}$ . As shown in the figure, using  $D_{\text{rms}} = D_{\text{ex}}$  in the RV simulations will give good agreement with the TD simulations only for restricted (and correlated) regions of distance and period. Both the BJ84 and the LP99 equations result in improvements over the case of no modification to  $D_{\text{rms}}$  and lead to values within about 10% of the TD simulations for periods ranging from less than about 1 s for M 4 to periods of about 100 s or even longer for M 8. The results from using the LP99 equation are the same as those from using the BJ84 equation for short periods, but they differ for longer periods, for which RV simulations using the LP99 equation are

closer to the TD simulations than are those from the RV simulations that use the BJ84 equation. Because engineering applications are often concerned with periods that are less than one or two seconds, Figure 5 suggests that the BJ84 and LP99 equations will give reasonable results in many cases. But the new equation (BT12) leads to a significant improvement in the RV simulations, compared to the BJ84 and LP99 computations, over a wide range of magnitudes, distances, and periods, and as the new equation is easy to implement, we recommend its use over the previous equations for determining  $D_{\text{rms}}$  in RV simulations.

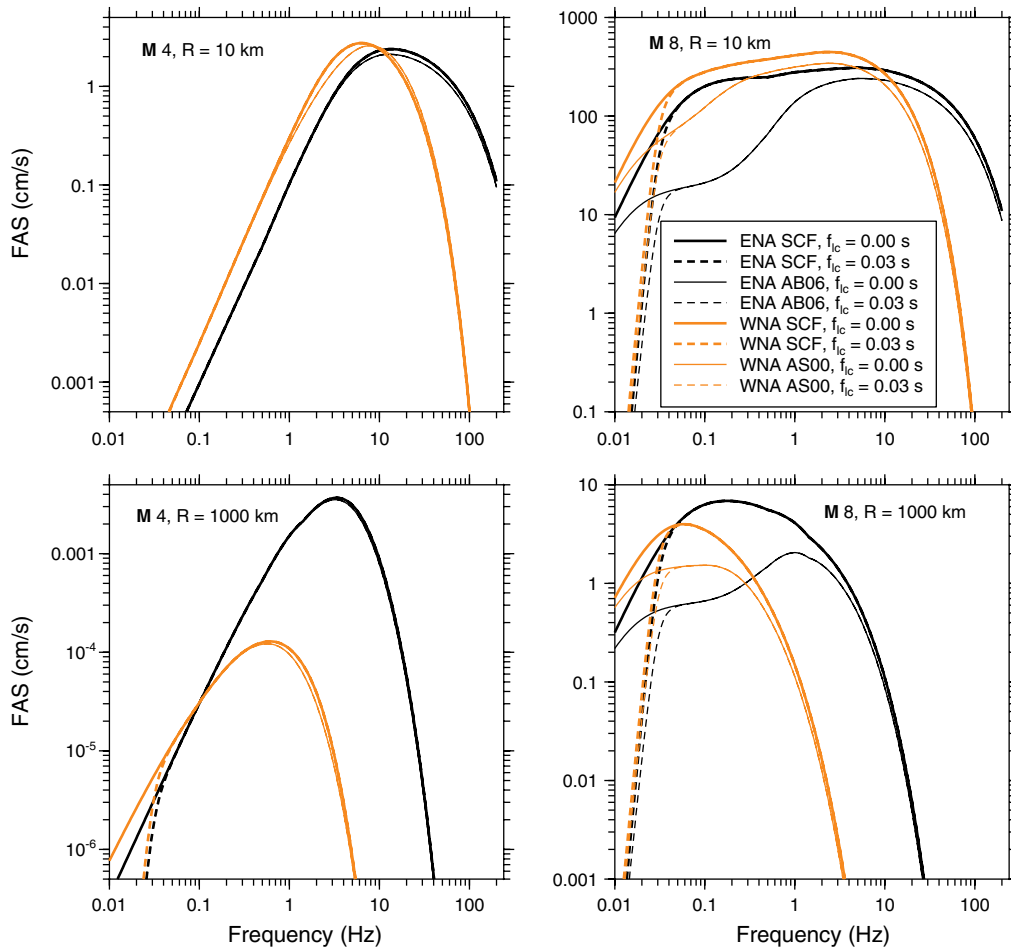


**Figure 6.** FAS for models used in this paper (see Table 1 and the [E](#) electronic supplement to this paper) for selected magnitudes and distances. The color version of this figure is available only in the electronic edition.

### Using $D_{\text{rms}}$ Computations in Models for Which the Coefficients Were Not Derived

The results in Figure 5 for the BT12 calculations are a consistency check to confirm that the computations were done correctly, because the coefficients in the equation for  $D_{\text{rms}}$  were designed to match the TD simulations for this model (the SCF ENA model, with no low-cut filter). The good agreement between the TD and RV simulations says nothing about the applicability of the BT12 coefficients used in Figure 5 for RV simulations based on other models. We address that in this section by comparing TD and RV simulations for other models for which the BT12 coefficients were not derived using equation (10) with the base-case ENA and WNA BT12 coefficients to compute  $D_{\text{rms}}$  in the RV simulations. We consider SCF and double-corner frequency models for both ENA and WNA (Table 1), and for each source model we consider two models, one with no low-cut filter and one with a low-cut filter of 0.03 Hz, for a total of eight models. The best way to appreciate the differences in the ground-motion models is to look at the Fourier acceleration spectra (FAS) for representative magnitudes and distances. These are shown in Figure 6.

The differences in low-frequency amplitudes for the ENA and WNA models are primarily due to the differences in geometrical spreading ( $1/R^{1.3}$  for ENA and  $1/R$  for WNA); these differences are not important for the RV versus TD comparison because geometrical spreading does not affect the shape of the FAS. Of much more importance are the other differences in the models, including whether the source spectra have one or two corner frequencies, the whole-path attenuation parameter  $Q(f)$ , and the high-frequency diminution parameter  $\kappa_0$ . This latter parameter is very different between the ENA and WNA models (0.005 s and 0.030 s, respectively), and this leads to the pronounced differences in the high-frequency FAS at close distances.

Comparisons of the RV and TD simulations for the ENA models that were not used in deriving the BT12 coefficients for ENA are shown in Figure 7. The top row of graphs is for the SCF model with a low-cut filter of 0.03 Hz. The mismatch between the TD and RV simulations is only important for periods greater than the filter period (33 s) and becomes increasingly important as the magnitude increases (because larger earthquakes have relatively more long-period energy than smaller earthquakes, and thus the long-period oscillator

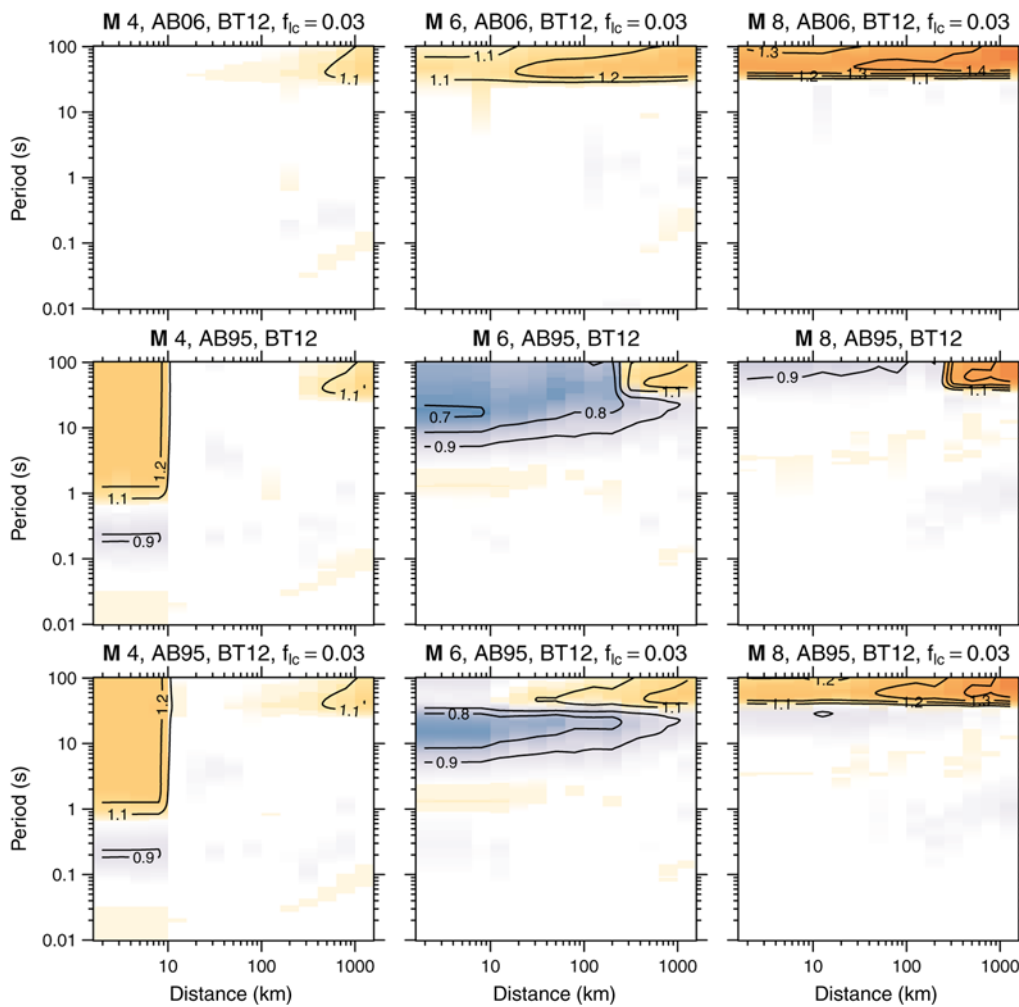


**Figure 7.** A shaded contour plot of the TD/RV ratios for various ENA models not used to derive the coefficients used in the BT12  $D_{rms}$  computations (see Table 1 and (E) the electronic supplement to this paper for model details). The base-case ENA BT12 coefficients were used in these comparisons. Top row: ENA SCF 250 bar model with a 0.03 Hz low-cut filter. Middle row: ENA AB95 two-corner model, no low-cut filter. Bottom row: ENA AB95 two-corner model, 0.03 Hz low-cut filter. The color version of this figure is available only in the electronic edition.

response will be more sensitive to low-cut filtering). The next two rows of graphs in Figure 7 are for the double-corner ENA model, without and with a low-cut filter, respectively. As before, the new modifications work well for shorter periods, with significant differences only for longer periods. The lesson from Figure 7 is that, for most cases of interest (periods less than about 10 s), the BT12 coefficients derived from the case of SCF without low-cut filtering work well. A similar conclusion holds for the WNA models (E see the electronic supplement to this paper, in which TD and RV ratios are shown for four models, similar to those used for ENA: SCF and double-corner frequency, without and with low-cut filtering).

A harsher test of the applicability of the new equation for  $D_{rms}$  is to use the equation with coefficients from the ENA model in RV predictions of motions for a WNA model, and vice versa (note that the spectral moments for the RV simulations will be computed from the correct ground-motion model; it is only the  $D_{rms}$  computation that mixes models).

These results are shown in the top two rows of Figure 8 for the SCF ENA and WNA models. Except for the smallest earthquake (at periods that increase with distance), the “wrong” coefficients work quite well. This led us to consider using an average of the  $D_{rms}$ ’s computed for the ENA and WNA coefficients in the RV simulations (i.e., BT12-combined); these results are shown in the bottom two rows of Figure 8. In general, the comparison with the TD simulations is now quite good. It clearly is impossible to sample all possible models, but we feel that these models encompass a wide range of the models currently in use.

## Discussion and Conclusions

Using TD and RV simulations for response spectra over a wide range of periods, magnitudes, and distances, we first evaluated existing equations to determine the duration ( $D_{rms}$ ) used to compute rms accelerations in RV stochastic-method simulations; these equations are from Boore and Joyner

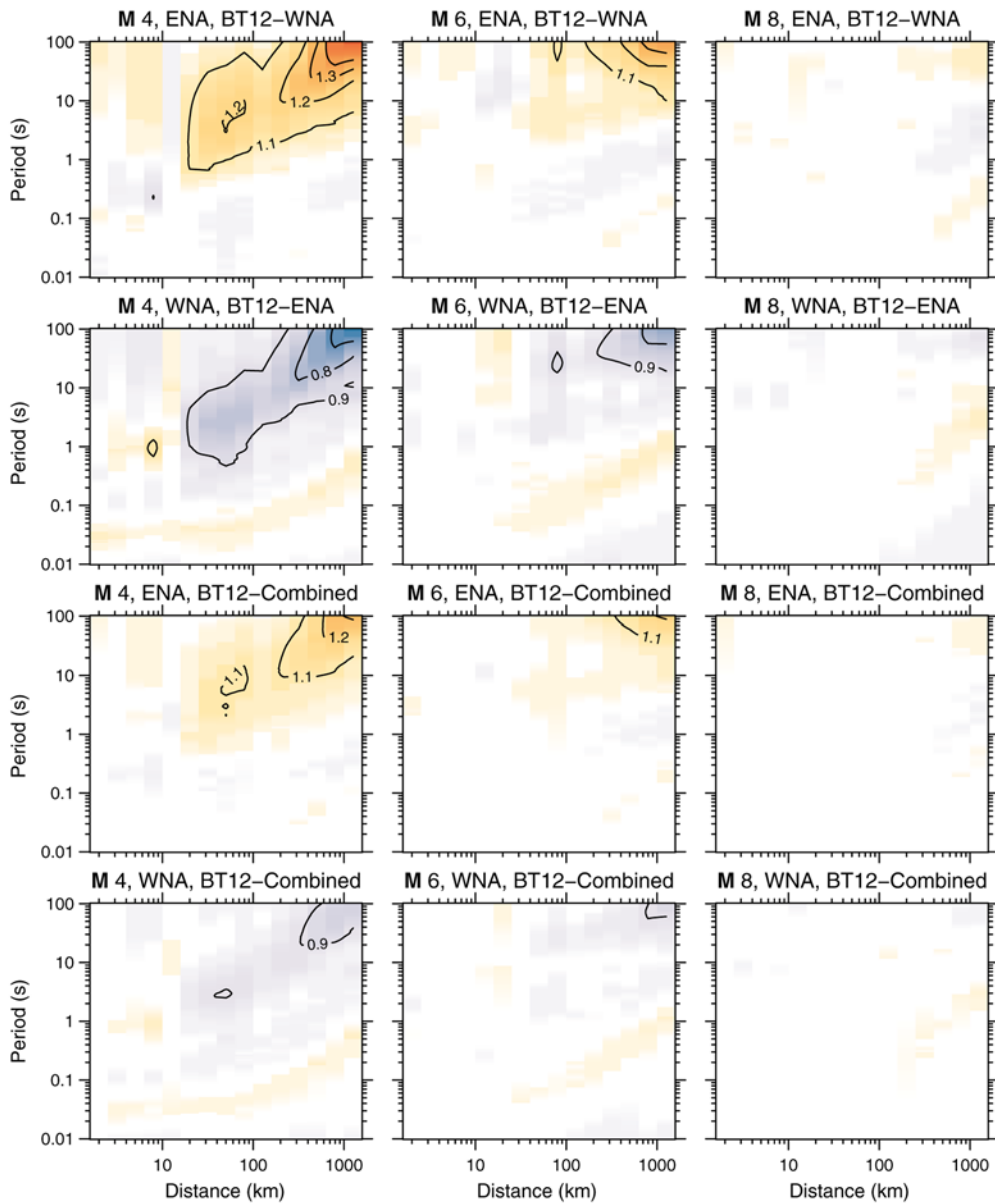


**Figure 8.** A shaded contour plot of the TD/RV ratios for various ENA and WNA models not used to derive the coefficients used in the BT12  $D_{\text{rms}}$  computations (see Table 1 and ⑤ the electronic supplement to this paper for model details). Top row: ENA SCF 250 bar model with no low-cut filter, using  $D_{\text{rms}}$  computed from the BT12 WNA coefficients. Second row: WNA SCF 100 bar model with no low-cut filter, using  $D_{\text{rms}}$  computed from the BT12 ENA coefficients. Third row: ENA SCF 250 bar model with no low-cut filter, using an average of  $D_{\text{rms}}$  computed from the BT12 ENA and WNA coefficients. Bottom row: WNA SCF 100 bar model with no low-cut filter, using an average of  $D_{\text{rms}}$  computed from the BT12 ENA and WNA coefficients. The color version of this figure is available only in the electronic edition.

(1984) and Liu and Pezeshk (1999). We found that the LP99 equation generally works better than that of BJ84, and that the RV simulations using the BJ84 and LP99 equations are within about 10% of the TD simulations for the magnitudes, distances, and periods of most engineering interest ( $M \gtrsim 5$ ,  $R \gtrsim 10$  km, and  $T \lesssim 2$  s for  $M 5$ , increasing to more than 100 s for  $M 8$ ). There is a considerable amount of variability in the ratio of TD to RV simulations in this range, however. To improve the RV simulations, we derived a new equation for the computation of  $D_{\text{rms}}$ . The new equation for  $D_{\text{rms}}$  leads to better agreement with TD simulations throughout

a large range of magnitudes, distances, periods, and seismological models than if the previous equations for  $D_{\text{rms}}$  are used in the RV simulations. The improvements are particularly effective for small magnitudes and long periods, but they also remove a small but persistent bias at short periods. Using the new equation adds only a negligible increase in the computational time; even with the new equation, the RV simulations are thousands of times faster than the TD simulations. A fundamental factor in the relatively long computational time for the TD simulations is that many simulations are needed to produce relatively smooth response spectra (we used 800

simulations for each magnitude and distance in this paper). In addition, the small value of the diminution parameter  $\kappa_0$  for the ENA models results in a richer content of high-frequency ground motions for ENA than for WNA, and this increased high-frequency content requires a much smaller time step in the ENA TD simulations, which substantially increases the time required to generate a time series (we use  $dt = 0.001$  s for ENA and  $dt = 0.005$  s for WNA).

The coefficient tables we provide for the computation of  $D_{\text{rms}}$  were generated for TD simulations using an exponential time window, rather than a box window (the BJ84 and LP99 modifications also used an exponential window), and the rms-to-peak factors used in the computations were those discussed in Boore (2003), from Cartwright and Longuet-Higgins (1956), rather than an alternative such as Der Kiureghian (1980). For consistency, any comparisons of TD and RV results should use these stochastic-model parameters.

Two sets of coefficients for the new equation for  $D_{\text{rms}}$  are provided: one for a standard ENA model and one for a standard WNA model. The models differ in many ways, the most important for this paper being the value of  $\kappa_0$ : 0.005 s for ENA and 0.030 s for WNA. Although the coefficients depend on the particular model for which they were derived, we find that in general the RV simulation results are not too sensitive to which set of coefficients is used. The exceptions to this are for very long periods, large distances, and small magnitudes, which do not control the hazard for most earthquake hazard analyses. We recommend using the set of coefficients from the model closest to the one under consideration. In particular, models with very small values of  $\kappa_0$  should use the ENA coefficients, while those with larger values should use the WNA coefficients. For intermediate values of  $\kappa_0$ , the average of the  $D_{\text{rms}}$ 's computed from the ENA and the WNA coefficients can be used in the RV simulations. Of course, it is good practice to spot check the RV and TD simulations for situations in which the ground-motion models are not similar to either of those used here.

### Data and Resources

The latest version of the SMSIM programs used for the simulations can be obtained from the online software link at <http://www.daveboore.com> (last accessed on October 2011); their use is described in Boore (2005). Version 3.29 (and higher) of SMSIM contains the coefficient files for the default  $D_{\text{rms}}$  coefficients (based on single-corner frequency eastern North America [ENA] and western North America [WNA] models, with no low-cut filter), and the random-vibration programs and parameter files have been modified to make use of these coefficients. The genetic algorithm calculations were done using the R package rgenoud (Mebane and Sekhon, 2011), which can be obtained from <http://www.r-project.org/> (last accessed on October 2011). A description of the Next Generation Attenuation–East (NGA-E) project is given in <http://peer.berkeley.edu/ngaeast/> (last accessed on October 2011), and the NGA-W2 task for developing damp-

ing modifications is discussed in <http://peer.berkeley.edu/ngawest2/tasks/task-6-damping-scaling/> (last accessed on October 2011).

### Acknowledgments

We thank John Douglas, Rob Graves, Jim Kalkanos, and two anonymous reviewers for their thoughtful comments and suggestions, and we thank Frank Scherbaum for pointing out a typographical error in one of our equations.

### References

- Abrahamson, N. A., P. Birkhauser, M. Koller, D. Mayer-Rosa, P. Smit, C. Sprecher, S. Tinic, and R. Graf (2002). PEGASOS: A comprehensive probabilistic seismic hazard assessment for nuclear power plants in Switzerland, in *Proc. 12th European Conference on Earthquake Engineering*, London, England, 9–13 September 2002, paper no. 633.
- Atkinson, G. M. (2004). Empirical attenuation of ground-motion spectral amplitudes in southeastern Canada and the northeastern United States, *Bull. Seismol. Soc. Am.* **94**, 1079–1095.
- Atkinson, G. M., and D. M. Boore (1995). Ground-motion relations for eastern North America, *Bull. Seismol. Soc. Am.* **85**, 17–30.
- Atkinson, G. M., and D. M. Boore (2006). Earthquake ground-motion prediction equations for eastern North America, *Bull. Seismol. Soc. Am.* **96**, 2181–2205.
- Atkinson, G. M., and W. Silva (2000). Stochastic modeling of California ground motions, *Bull. Seismol. Soc. Am.* **90**, 255–274.
- Boore, D. M. (1983). Stochastic simulation of high-frequency ground motions based on seismological models of the radiated spectra, *Bull. Seismol. Soc. Am.* **73**, 1865–1894.
- Boore, D. M. (2003). Simulation of ground motion using the stochastic method, *Pure Appl. Geophys.* **160**, 635–676.
- Boore, D. M. (2005). SMSIM—Fortran programs for simulating ground motions from earthquakes: Version 2.3—A revision of OFR 96-80-A, U.S. Geological Survey Open-File Report, *U. S. Geol. Surv. Open-File Rept. 00-509*, 55 pp.
- Boore, D. M. (2009). Comparing stochastic point-source and finite-source ground-motion simulations: SMSIM and EXSIM, *Bull. Seismol. Soc. Am.* **99**, 3202–3216.
- Boore, D. M., and W. B. Joyner (1984). A note on the use of random vibration theory to predict peak amplitudes of transient signals, *Bull. Seismol. Soc. Am.* **74**, 2035–2039.
- Cameron, W. I., and R. A. Green (2007). Damping correction factors for horizontal ground-motion response spectra, *Bull. Seismol. Soc. Am.* **97**, 934–960.
- Cartwright, D. E., and M. S. Longuet-Higgins (1956). The statistical distribution of the maxima of a random function, *Proc. Roy. Soc. Lond. Math. Phys. Sci.* **237**, 212–232.
- Der Kiureghian, A. (1980). Structural response to stationary excitation, *J. Eng. Mech. Div.* **EM6**, 1195–1213.
- Liu, L., and S. Pezeshk (1999). An improvement on the estimation of pseudoresponse spectral velocity using RVT method, *Bull. Seismol. Soc. Am.* **89**, 1384–1389.
- Mebane, W. R., Jr., and J. S. Sekhon (2011). Genetic optimization using derivatives: The rgenoud package for R, *J. Statist. Software* **42**, 1–26.
- Raof, M., R. B. Herrmann, and L. Malagnini (1999). Attenuation and excitation of three-component ground motion in Southern California, *Bull. Seismol. Soc. Am.* **89**, 888–902.
- Renault, P., S. Heuberger, and N. A. Abrahamson (2010). PEGASOS Refinement Project: An improved PSHA for Swiss nuclear power plants, in *Proceedings of the 14th European Conference on Earthquake Engineering*, Ohrid, Macedonia, 30 August–3 September 2010, paper no. 991.
- Saragoni, G. R., and G. C. Hart (1974). Simulation of artificial earthquakes, *Earthq. Eng. Struct. Dynam.* **2**, 249–267.

Scherbaum, F., F. Cotton, and H. Staedtke (2006). The estimation of minimum-misfit stochastic models from empirical ground-motion prediction equations, *Bull. Seismol. Soc. Am.* **96**, 427–445, doi [10.1785/0120050015](https://doi.org/10.1785/0120050015).

Tufts University  
113 Anderson Hall  
Medford, Massachusetts 02155  
[eric.thompson@tufts.edu](mailto:eric.thompson@tufts.edu)  
(E.M.T.)

U.S. Geological Survey  
MS 977  
345 Middlefield Road  
Menlo Park, California 94025  
[boore@usgs.gov](mailto:boore@usgs.gov)  
(D.M.B.)

Manuscript received 4 September 2011